

PROCEEDINGS OF SPIE

[SPIDigitalLibrary.org/conference-proceedings-of-spie](https://spiedigitallibrary.org/conference-proceedings-of-spie)

Quantization of static domains in slim superlattices

Averin, Dmitri, Korotkov, Alexander, Likharev, Konstantin

Dmitri V. Averin, Alexander N. Korotkov, Konstantin K. Likharev, "Quantization of static domains in slim superlattices," Proc. SPIE 1676, Advanced Semiconductor Epitaxial Growth Processes and Lateral and Vertical Fabrication, (2 September 1992); doi: 10.1117/12.137659

SPIE.

Event: Semiconductors '92, 1992, Somerset, NJ, United States

Quantization of static domains in slim superlattices

D.V. Averin,^(1,2) A.N. Korotkov,⁽²⁾ and K.K. Likharev^(1,2)

⁽¹⁾ Department of Physics, State University of New York, Stony Brook, NY 11794, USA
and

⁽²⁾ Department of Physics, Moscow State University, Moscow 119899 GSP, Russia

ABSTRACT

We have calculated dc $I-V$ curves of the semiconductor superlattices of a very small (practically, submicron) cross-section. The $I-V$ curves exhibit periodic oscillations with a voltage period e/C . These oscillations are caused by quantization of electric charge Q of the walls of static high-field domains.

2. INTRODUCTION

At sufficiently low temperatures, electron transport properties of small conductors separated by low-transparent tunnel barriers are dominated by single-electron charging effects.^{1,2} The origin of these effects is the quantization of electric charge Q of the electrodes in units of the fundamental charge e . In electrodes with small electric capacitance C , the charge quantization gives rise to the energy gaps (of the order of characteristic charging energy $E_c \equiv e^2/2C$) between states which differ by one extra electron in the conductor. Since these gaps can be varied continuously, for example, by externally applied voltages, one can control the motion of single electrons in such systems.

Single-electron charging effects were studied mostly in metallic systems. In semiconductor nanostructures, only double-barrier structures ("quantum dots" and "quantum wells") were investigated both experimentally³⁻⁶ and theoretically⁷⁻⁹. In this work we consider single-electron charging effects in multi-barrier superlattices (Fig. 1a).

3. BASIC RELATIONS

Let us consider a superlattice with narrow minibands. If the temperature T or Fermi energy drops eV_j across the barriers of the superlattice are larger than the miniband width δ ($\max\{T, eV_j\} \gg \delta$), electrons are nearly localized in the conducting layers, and electron motion through the superlattice can be described as sequential hopping. If an area S of the superlattice is small, electric capacitance C between nearest conducting layers in the superlattice can be also small in the sense that $T \ll e^2/C$. In such a "slim" superlattice with localized electrons, quantization of electric charge Q of its conducting layers becomes essential, since addition of even one electron to a conducting layer increases electrostatic energy of this layer considerably.

As in the double-barrier systems,^{10,11,6} charge quantization in the conducting layers may coexist with quantization of electron energy due to lateral confinement. When electrons occupy only the lowest miniband, the ratio Δ/E_c of the average spacing Δ between electron energy levels and charging energy E_c is independent of the area S as long as characteristic lateral dimensions of the superlattice is much larger than its period d . This ratio depends only on d , $\Delta/E_c \simeq a_B/d$,⁷ where a_B is the Bohr radius ($a_B \simeq 10\text{nm}$ for GaAs). In this work, we discuss the superlattices with $d \gg a_B$, where the discreteness of the energy

spectrum of the conducting layers is negligible. Besides this, we assume that equilibrium concentration of electrons in the conducting layers is sufficiently large, so that the total number of electrons in each layer is much larger than unity.

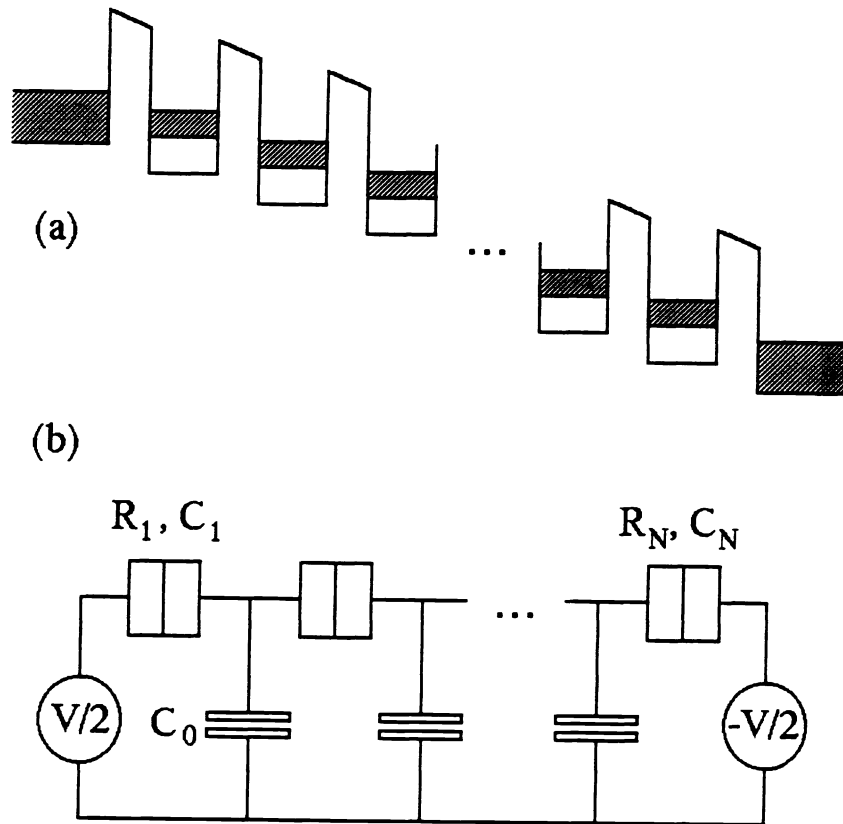


Fig. 1. (a) Conduction band edge profile of the multibarrier superlattice and (b) equivalent circuit of the superlattice. Dashed regions denote energy states occupied by electrons. Divided rectangle is the standard notation for a small-area tunnel junction.²

Under these conditions the superlattice is equivalent to a 1D array of metallic tunnel junctions¹². Specifically, in the superlattices with large barrier resistances R ($R \gg R_Q \equiv \pi\hbar/2e^2$) dynamics of electron tunneling is dominated by transitions in which electron tunnels through one barrier. This dynamics can be described by the standard master equation for probabilities $\sigma(n_1, \dots, n_i, \dots, n_{N-1}) \equiv \sigma\{n\}$ to find n_i extra electrons in the i th conducting layer:

$$\dot{\sigma}\{n\} = \sum_{j=1}^N [\Gamma_j^+ \{n\}_j^+ \sigma\{n\}_j^- + \Gamma_j^- \{n\}_j^- \sigma\{n\}_j^+ - (\Gamma_j^+ \{n\} + \Gamma_j^- \{n\}) \sigma\{n\}]. \quad (1)$$

Here Γ_j^\pm are the rates of forward and backward electron tunneling through the j th barrier, and by $\{n\}_j^\pm$ we denote the distribution of electron which differs from the distribution $\{n\}$ by the forward or backward tunneling of one electron through the j th barrier: $\{n\}_j^\pm \equiv \{n_1, \dots, n_j \mp 1, n_{j+1} \pm 1, \dots, n_{N-1}\}$.

The rates of electron tunneling through the j th barrier of the superlattice can be presented in the same

form as in metallic systems^{1,2}:

$$\Gamma_j = \frac{I_j(U_j/e)}{e} [1 - \exp\{-\frac{U_j}{T}\}]^{-1}, \quad (2)$$

where $I_j(V)$ is the dc $I-V$ curve of the barrier at a fixed dc voltage V across the barrier, while U_j is a decrease of electrostatic energy of the system due to the tunneling event. (In all numerical examples below we assume that temperature is small, $T \ll U_j$, and that the superlattice is uniform, $I_j(V) \equiv I_0(V)$.)

The energy U_j in eq. (2) can be expressed via the voltages across the j th barrier before ($V_j^{(i)}$) and after ($V_j^{(f)}$) the tunneling event:

$$U_j = \frac{e}{2}(V_j^{(i)} + V_j^{(f)}). \quad (3)$$

In general, these voltages should be calculated from the equivalent circuit shown in Fig. 1b. However, since the period of the superlattice is much smaller than its lateral dimensions, the self-capacitance C_0 of the conducting layers is also small, $C_0 \ll C$, and can be neglected for superlattices with not too large number N of periods,¹² $N < (C/C_0)^{1/2}$. For negligible C_0 we have:

$$U_j = e(V_j^{(i)} - \frac{e}{2C_{eff}}), \quad C_{eff} = C(1 + \frac{1}{N}). \quad (4)$$

The main difference with system of metallic junctions is the shape of the barrier $I-V$ curves $I_0(V)$, which for superlattice may contain negative differential resistance (NDR) region. For voltages smaller than the Fermi level μ in the conducting layers and energy gap above the lowest miniband, they can be approximated as follows:¹³

$$I_0(V) = \frac{V}{R} \left(\frac{1}{1 + (V/V_0)^2} + \lambda \right). \quad (5)$$

Here the first term describes tunneling which does not change the electron state with respect to motion along the layers of the superlattice, while the small parameter λ accounts for tunneling which is accompanied by scattering between these states, and determines the upper voltage boundary $V_0/\sqrt{\lambda}$ of the NDR region (the lower boundary of this region is approximately V_0).

4. HIGH-FIELD DOMAINS

In conventional superlattices with large areas, the potential e/C associated with one electron in the conducting layer is much smaller than characteristic voltage scale V_0 of the barrier $I-V$ curve (1). In this case, different tunneling events in the superlattice are virtually not correlated, and the master equation (1) is reduced to an equation for average current between conducting regions and their average potentials. This equation corresponds to representation of the superlattice¹⁴ as a series of capacitances shunted by non-linear resistances. This model is sufficient for description of the high-field domain formation¹⁵⁻¹⁸ in the superlattice.

If the bias voltage V across the superlattice exceeds NV_0 , at least one of the barriers is biased in the NDR region, and uniform potential distribution along the superlattice becomes unstable. A transient leads to another state in which nearly all voltage drops across one junction ("high-field domain") - see Fig. 2. The domain is the bottleneck for the current flow, and dc current I through the superlattice decreases due to domain formation. In superlattices with small λ ($\lambda < N^{-2}$) the tunnel barrier in the domain is biased in the NDR region of its $I-V$ curve, so that there is a voltage region where the current through the superlattice decreases smoothly with increasing voltage. At larger λ ($\lambda > N^{-2}$) such a region is absent

and formation of the high-field domain shows up as an abrupt transition between two current branches of the superlattice $I-V$ curve with increasing current. These two types of behavior are illustrated in Fig. 3.

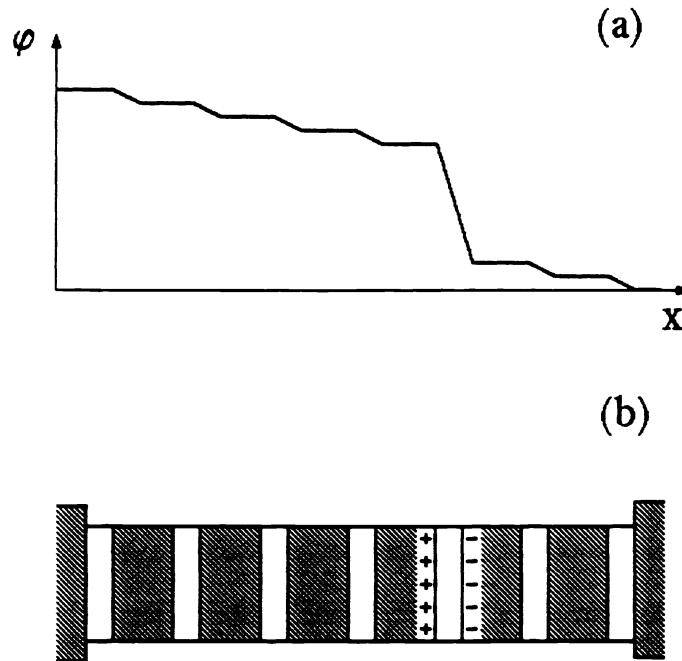


Fig. 2. Schematic distribution of electrostatic potential (a) and electric charge (b) along the superlattice with one high field domain.

In both cases an increase of the current I leads eventually (at $I \simeq V_0/2R$) to formation of the second high-field domain, the third domain, etc. The process of domains formation continues almost periodically in the bias voltage, with the period about $(N + 2/\lambda)V_0$. This results in the periodic oscillations of the dc current in the superlattice with this period, similar to those shown in Fig. 3b. (For parameters of Fig. 3a the period is too large to be seen in this figure.) The total number of oscillations is equal to the number of periods in the superlattice.

Another feature associated with high-field domain formation is the hysteresis in the dc $I-V$ curves of the superlattice. When the voltage increases, domains are formed at larger voltages than those at which they are destroyed at decreasing voltage, so that the current depends on the history of voltage variations. Such a hysteresis can be seen in Fig. 3a. At not too small ratios $(e/C)/V_0$, voltage fluctuations due to shot noise caused by electron tunneling, lead to rapid switching between possible current values, and actual dc $I-V$ curve passes somewhere in between them.

The above two features are typical experimental manifestations of high-field domains in superlattices.¹⁵⁻¹⁸

5. DOMAIN QUANTIZATION

The single-electron voltage e/C is inversely proportional to the superlattice area, and at sufficiently small areas can become larger than the voltage scale V_0 of the barrier $I-V$ curve (5). In this case, discreteness of electric charge of conduction layers becomes essential. Figures 4,5 show the dc $I-V$ curves of the superlattices in this regime, calculated by numerical simulation of dynamics of electron tunneling

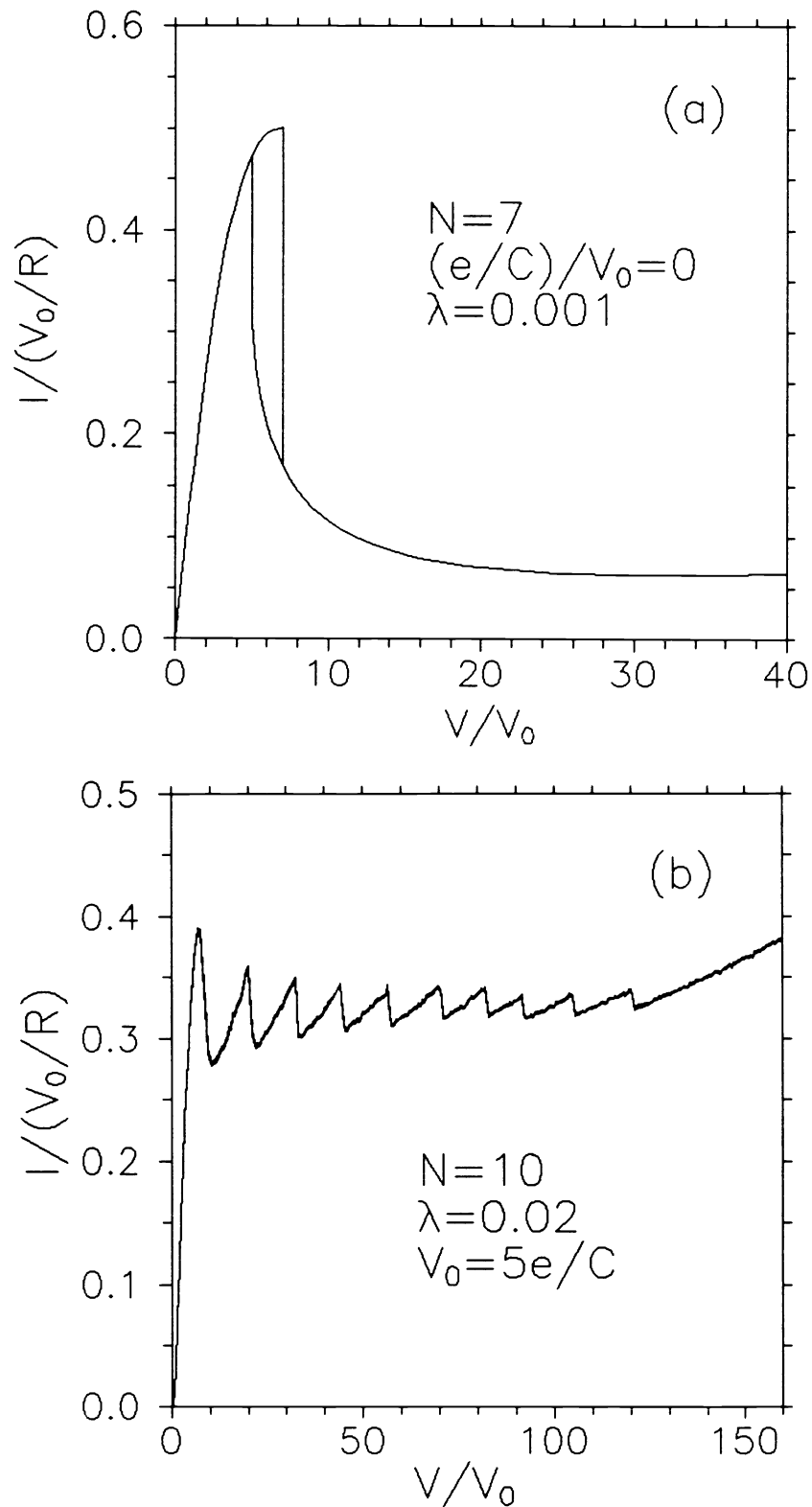


Fig. 3. The DC $I-V$ curves of conventional large-area superlattice, calculated by numerical modeling of dynamics of electron tunneling based on eqs. (2)-(5). The curves reflect formation of the high-field domains in the superlattice.

based on eqs. (2)-(5). The most obvious manifestation of single-electron charging effects is Coulomb blockade^{1,2}, i.e. suppression of current at small voltages $V < V_t$ (eq. (4) shows that Coulomb blockade threshold V_t is $(N - 1)e/2C$).

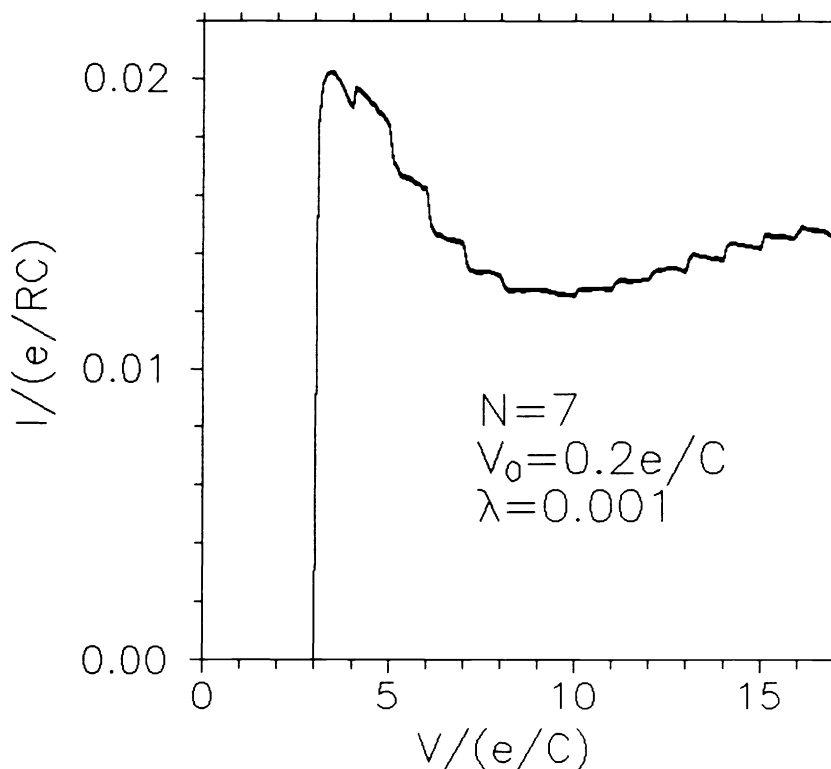


Fig. 4. The DC $I-V$ curve of a slim superlattice with the same set of parameters as in Fig. 2a, except for the area, i.e. $(e/C)/V_0$ ratio. The curve exhibits single-electron charging effects - see text.

At voltages just above Coulomb blockade threshold, electron tunneling events in different barriers of the superlattice are correlated. Similar to the 1D arrays of metallic junctions,¹⁹ such a correlated motion of electrons through the superlattice should give rise to SET oscillations with the frequency $f = I/e$. However, the amplitude of the SET oscillations in the limit of small C_0 is proportional to $N(C_0/C)^{1/2}$ and can be small for short superlattices.

The new feature of the superlattice $I-V$ curves (in comparison to the 1D arrays of metallic tunnel junctions) is periodic oscillation of the current with voltage period e/C - see Figs. 4,5. The origin of this effect is quantization of the voltage drop ΔV across the high-field domain barrier. Since this barrier is the bottleneck for the current flow, the current in the superlattice is determined by ΔV . Due to the discreteness of the charge in the conducting layers adjacent to the barrier, ΔV increases in a stepwise manner with increasing bias voltage across the superlattice. Each step in this dependence corresponds to addition of one extra electron to these layers. (This picture resembles that describing formation of Coulomb staircase in the dc $I-V$ curves of the metallic double-junction system.^{1,2})

Quantitatively, at small λ the tunneling rate through the high-field domain barrier is much smaller than that through other barriers of the superlattice. As a result, electrons are accumulated in the conducting

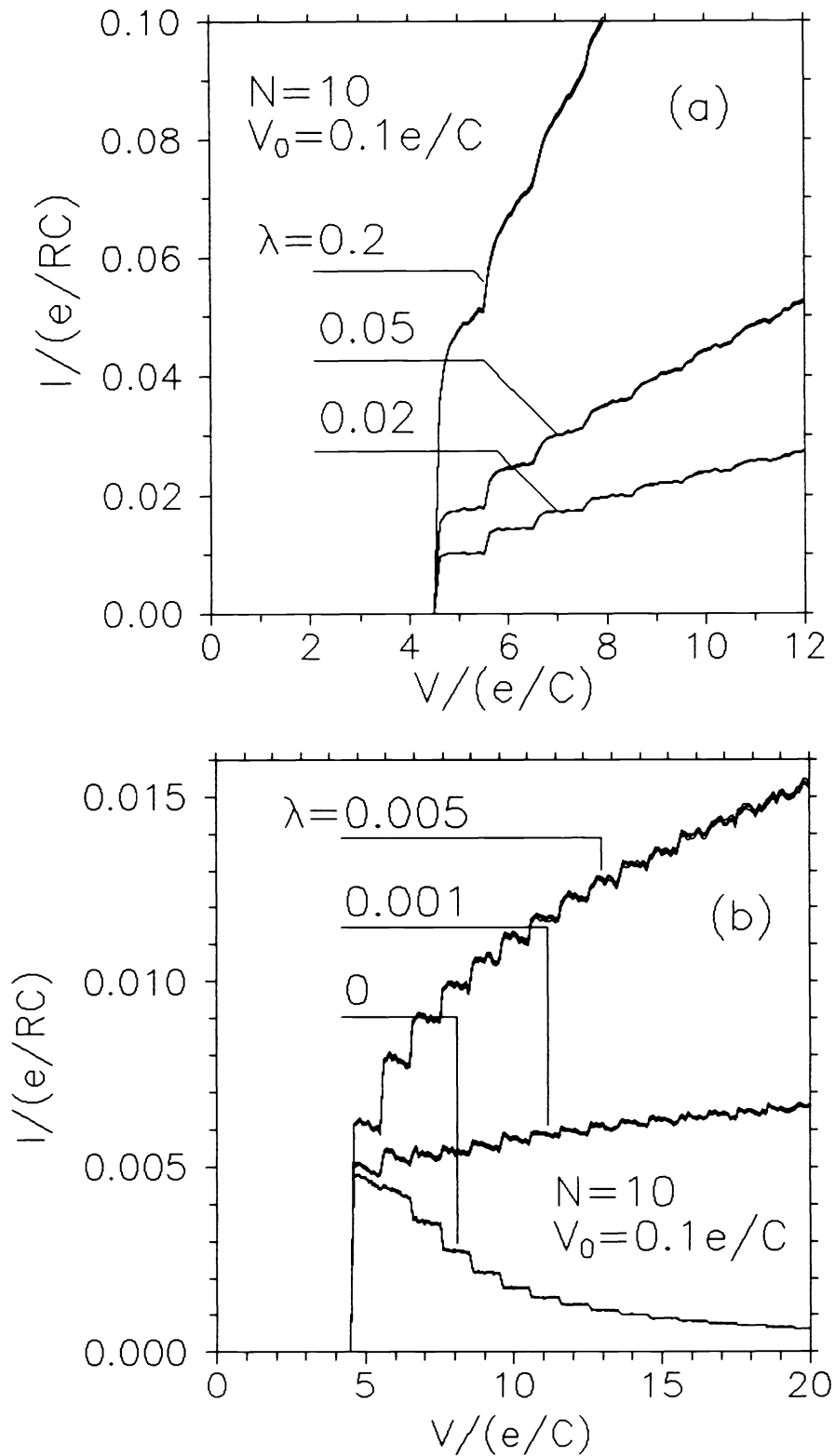


Fig. 5. Evolution of the current oscillations in the dc $I - V$ curves of the slim superlattice with increasing Ohmic contribution to the barrier current.

layers adjacent to this barrier and

$$\Delta V = \frac{1}{N}(V + (N - 1)\frac{ne}{C}), \quad (6)$$

where n is the number of accumulated electrons. In the adopted approximation the current in the superlattice is determined solely by ΔV :

$$I = I_0(\Delta V - \frac{e}{2C_{eff}}) = I_0(\frac{1}{N}(V - V_t + (N - 1)\frac{ne}{C})). \quad (7)$$

The voltage drop across the other barriers of the superlattice is

$$\delta V = \frac{1}{N}(V + (N - 1)\frac{ne}{C}). \quad (8)$$

Electron can enter the superlattice and increase n by one if $\delta V > V_t$. This means that

$$n = \text{Int}[(V - V_t)C/e] + 1. \quad (9)$$

Equations (7) and (9) imply that at sufficiently small λ ($\sqrt{\lambda} \ll V_0/(e/C)$) the current I exhibits staircase-like "fine" structure with the period e/C , while the general shape of the $I-V$ curve (at voltages not too close to the Coulomb blockade threshold) follows that of a single barrier. This situation is illustrated by Fig. 4 and the lowest curve in Fig. 5. At larger λ the $I-V$ curve deviates from $I_0(V)$, but the fine structure persists until $\lambda \simeq V_0/(e/C)$, when it becomes considerably less pronounced -see Fig. 5.

The voltage period e/C of the current modulation in the superlattice with large space period considered above is determined by the charge discreteness. If the space period of the superlattice is comparable to the Bohr radius, the discreteness of the energy spectrum of the conducting layers should become essential - see Sec. 2. The energy discreteness should modify the voltage period in the same way as in the double-barrier system.⁷

Even more interesting question is the crossover between sequential hopping of electrons in the superlattice, which is dominated by the single-electron charging effects, and coherent electron wave propagation in the lowest Bloch miniband. These two regimes of electron transport are characterized, respectively, by the SET oscillations with frequency I/e , and by the Bloch oscillations with frequency $eV/\hbar N$. Crudely, the crossover should take place at $E_c \simeq \Delta$. However, its quantitative picture is far from being clear at present.

6. CONCLUSION

To summarize, we have shown that in the "slim" superlattices, static high-field domains should be quantized, giving rise to periodic oscillations of the dc current in the superlattice. Such a quantization can be realized in the superlattices with narrow minibands, provided that the voltage e/C associated with a single electron is larger than the lower voltage boundary V_0 of the NDR region in the barrier $I-V$ curves. This condition presumably can be satisfied in the superlattices with effective area below $(0.1\mu\text{m})^2$ and period larger than 10 nm, for which $e/C > 1$ mV.

ACKNOWLEDGMENTS

Useful discussions with M. Reed are gratefully acknowledged. This work was supported by AFOSR Grant No. 91-0445.

REFERENCES

1. D.V. Averin and K.K. Likharev, in: *Mesoscopic Phenomena in Solids*, ed. by B. Altshuler *et al.* (Elsevier, Amsterdam, 1991), p. 173.
2. *Single Charge Tunneling*, ed. by H. Grabert and M.H. Devoret (Plenum, New York, 1992), to be published.
3. U. Meirav, M.A. Kastner, and S.J. Wind, *Phys. Rev. Lett.* **65**, 771 (1990).
4. L.P. Kouwenhoven, N.C. van der Vaart, A.T. Johnson, W. Kool, C.J.P.M. Harmans, J.G. Williamson, A.A.M. Staring, and C.T. Foxon, *Z. Phys. B* **85**, 367 (1991).
5. D.C. Glattli, C. Pasquier, U. Meirav, F.I.B. Williams, Y. Jin, and B. Etienne, *Z. Phys. B* **85**, 375 (1991).
6. Bo Su, V.J. Goldman, and J.E. Cunningham, *Science* **255**, 313 (1992).
7. D.V. Averin, A.N. Korotkov, and K.K. Likharev, *Phys. Rev. B* **44**, 6199 (1991).
8. C.W.J. Beenakker, *Phys. Rev. B* **44**, 1646 (1991).
9. A. Groshev, T. Ivanov, V. Valtchinov, *Phys. Rev. Lett.* **66**, 1082 (1991).
10. D.V. Averin and A.N. Korotkov, *J. Low Temp. Phys.* **80**, 173 (1990).
11. P.L. McEuen, E.B. Foxman, U. Meirav, M.A. Kastner, Y. Meir, N.S. Wingreen, and S.J. Wind, *Phys. Rev. Lett.* **66**, 1926 (1991).
12. K.K. Likharev, N.S. Bachvalov, G.S. Kazacha, and S.I. Serduykova, *IEEE Trans. Magn.* **25**, 1436 (1989).
13. E.S. Borovitskaya and V.M. Genkin, *Sov. Phys. Solid State* **27**, 475 (1985); **29**, 1174 (1987).
14. B. Laikhtman, *Phys. Rev. B* **44**, 11260 (1991).
15. L. Esaki and L.L. Chang, *Phys. Rev. Lett.* **33**, 495 (1974).
16. K.K. Choi, B.F. Levine, R.J. Malik, J. Walker, and C.G. Bethea, *Phys. Rev. B* **35**, 4172 (1987).
17. Y. Kawamura, K. Wakita, and K. Oe, *Jap. J. Appl. Phys.* **26**, L1603 (1987).
18. T.H.H. Vuong, D.C. Tsui, and W.T. Tsang, *J. Appl. Phys.* **66**, 3688 (1989).
19. P. Delsing, K.K. Likharev, L.S. Kuzmin, and T. Claeson, *Phys. Rev. Lett.* **63**, 1861 (1989).